Science Bulletin 67 (2022) 2550–2556

Contents lists available at ScienceDirect

Science Bulletin

journal homepage: www.elsevier.com/locate/scib

Article

Probing quantum many-body correlations by universal ramping dynamics

Libo Liang [a,1], Wei Zheng [b,c,1], Ruixiao Yao [d,1], Qinpei Zheng [a], Zhiyuan Yao [e], Tian-Gang Zhou [e], Qi Huang [a], Zhongchi Zhang [d], Jilai Ye [d], Xiaoji Zhou [a], Xuzong Chen [a,*], Wenlan Chen [d,f,*], Hui Zhai [e,*], Jiazhong Hu [d,f,*]

[a] School of Electronics, Peking University, Beijing 100871, China
[b] Hefei National Laboratory for Physical Sciences at the Microscale and Department of Modern Physics, University of Science and Technology of China, Hefei 230026, China
[c] CAS Center for Excellence in Quantum Information and Quantum Physics, University of Science and Technology of China, Hefei 230026, China
[d] Department of Physics and State Key Laboratory of Low Dimensional Quantum Physics, Tsinghua University, Beijing 100084, China
[e] Institute for Advanced Study, Tsinghua University, Beijing 100084, China
[f] Frontier Science Center for Quantum Information, Beijing 100084, China

ARTICLE INFO

Article history:
Received 19 August 2022
Received in revised form 8 November 2022
Accepted 1 December 2022
Available online 5 December 2022

Keyword:
Ramping dynamics
Many-body correlations
Optical lattices
Degenerate quantum gas

ABSTRACT

Ramping a physical parameter is one of the most common experimental protocols in studying a quantum system, and ramping dynamics has been widely used in preparing a quantum state and probing physical properties. Here, we present a novel method of probing quantum many-body correlation by ramping dynamics. We ramp a Hamiltonian parameter to the same target value from different initial values and with different velocities, and we show that the first-order correction on the finite ramping velocity is universal and path-independent, revealing a novel quantum many-body correlation function of the equilibrium phases at the target values. We term this method as the non-adiabatic linear response since this is the leading order correction beyond the adiabatic limit. We demonstrate this method experimentally by studying the Bose-Hubbard model with ultracold atoms in three-dimensional optical lattices. Unlike the conventional linear response that reveals whether the quasi-particle dispersion of a quantum phase is gapped or gapless, this probe is more sensitive to whether the quasi-particle lifetime is long enough such that the quantum phase possesses a well-defined quasi-particle description. In the Bose-Hubbard model, this non-adiabatic linear response is significant in the quantum critical regime where well-defined quasi-particles are absent. And in contrast, this response is vanishingly small in both superfluid and Mott insulators which possess well-defined quasi-particles. Because our proposal uses the most common experimental protocol, we envision that our method can find broad applications in probing various quantum systems.

1. Introduction

Quantum many-body systems display rich phenomena characterized by varieties of correlations, and many experimental tools have been developed to probe these correlations. These methods include various spectroscopies and transport measurements in both condensed matter systems [1–3] and ultracold atomic systems [4,5]. These probes can measure quasi-particle dispersions and reveal whether a quantum phase possesses a charge gap or spin gap, with the help of the linear response theory. For instance, possessing a gap or not is an important way to characterize quantum many-body correlations and distinguishes different phases.

There is also another important aspect of quantum many-body correlations, that is, whether the quasi-particle lifetime is long enough such that a quantum phase possesses a well-defined quasi-particle description or not [6]. It is a different characterization of quantum phases, compared with gap or gapless feature in the dispersion. Quantum phases, such as conventional metals, band insulators, and Bose or Fermi superfluids, have well-defined quasi-particles. Among them, some are gapless, such as metals and Bose superfluids. And some are gapped, for instance, *s*-wave fermion paired superfluids have spin gaps and band insulators have charge gaps. Quantum phases, such as states in quantum critical regimes [6], Luttinger liquids in one-dimension [7] and non-Fermi liquids [8,9], do not have well-defined quasi-particle descriptions.

* Corresponding authors.
E-mail addresses: xuzongchen@pku.edu.cn (X. Chen), cwlaser@ultracold.cn (W. Chen), hzhai@mail.tsinghua.edu.cn (H. Zhai), hujiazhong01@ultracold.cn (J. Hu).
[1] These authors contributed equally to this work.

https://doi.org/10.1016/j.scib.2022.12.005
2095-9273/

In both condensed matter and ultracold atomic systems, spectroscopy measurements can always determine the entire spectral function [1,2,4,5,10–16]. Once the entire spectral function is known, it becomes clear whether a system is gapped or whether the system has a well-defined quasi-particle description. However, such measurements require scanning all frequency ranges in the relevant energy scale. For many properties, there is a more direct measurement that is less involved. A typical example is the charge gap. A dc transport experiment can immediately tell whether the system has a charge gap without knowing the complete information of the spectral function. This work will propose a similar shortcut to measure whether the system has well-defined quasi-particle behaviors, probing via ramping dynamics in many-body systems.

Ramping a physical parameter is one of the most widely-used control protocols in studying a quantum system. When the ramping rate is slow enough, the quantum state can follow the change of parameters adiabatically and retain the ground state of the instantaneous Hamiltonian at a given time. This protocol has been widely used in preparing a quantum state with high fidelities and adiabatic quantum computations. When the ramping rate is non-negligible, the system is brought into a non-equilibrium situation that deviates from the instantaneous ground state and generates excitations. In this situation, the ramping protocol can be turned into a probing scheme, and two of the most well-known examples are the Thouless pumping [17–20] and the Kibble-Zurek mechanism [21–31]. For the Thouless pumping, the accumulated charge is quantized after a pumping cycle, and this quantized charge probes the topological invariant of the equilibrium phase [17–20]. For the Kibble-Zurek mechanism, topological defects are excited when a parameter is ramped across an equilibrium phase transition point, and the dependence of topological defect numbers on ramping rates reveals the critical exponent of the equilibrium phase transition [21–31].

Here we present a novel scheme of probing quantum many-body correlations by ramping dynamics, with both theoretical frameworks and experimental results. Our scheme utilizes the first-order correction on finite ramping rates beyond the adiabatic limit, and therefore, we term it as *the non-adiabatic linear response*. Remarkably, we show that the response is independent of the history of the ramping trajectories and only depends on the ending point of the ramping. In other words, our scheme probes the universal aspects instead of the details of the ramping dynamics. Moreover, the universal quantity deduced from this response can be attributed to an equilibrium quantum many-body correlation function at the ending point. Unlike the Thouless pumping and the Kibble-Zurek mechanism, the correlation function revealed by this method is quite general, not limited to topology or criticality. We investigate this scheme numerically in three different models as examples, the transverse field Ising model, the fermion pairing model, and the Bogoliubov model for bosons. We also demonstrate this scheme experimentally by studying the Bose-Hubbard model using degenerate bosonic atoms in optical lattices. In the Bose-Hubbard model, we show theoretically and experimentally that this response is significant in the quantum critical regime without well-defined quasi-particles and is vanishingly small in the superfluid phase (gapless) and the bosonic Mott insulator phase (gapped), both of which possess well-defined quasi-particle descriptions. Therefore, our results show that this response can be sensitive to whether the quantum phases possess well-defined quasi-particle descriptions rather than whether their quasi-particle dispersions are gapless or gapped.

2. Theoretical framework

Let's consider a Hamiltonian $\widehat{H}(\lambda)$ that depends on a parameter λ, and a time-dependent ramping of the parameter $\lambda(t)$ from λ_i to λ_f. We start with the ground state at λ_i and we choose $\lambda(t)$ that satisfies (1) $\partial\lambda/\partial t|_{\lambda_\mathrm{i}} = 0$; (2) $\partial\lambda/\partial t|_{\lambda_\mathrm{f}} = v$; and (3) the absolute value of $\partial\lambda/\partial t$ is always bounded by v for the entire ramping duration. As soon as λ reaches λ_f, we immediately measure an observable $\langle\widehat{O}\rangle$. Suppose we repeat the measurements with different ramping trajectories, by choosing different initial state at different λ_i and different ramping velocities, as shown in Fig. 1a, and then we plot $\langle\widehat{O}\rangle$ as a function of the velocity v, as schematically shown in Fig. 1b. We can make a series expansion of $\langle\widehat{O}\rangle$ in term of v as (See Fig. 2)

$$\langle\hat{O}\rangle = \langle\lambda_\mathrm{f}|\hat{O}|\lambda_\mathrm{f}\rangle + \alpha v + \ldots \tag{1}$$

Here $|\lambda\rangle$ denotes the instantaneous ground state of $\widehat{H}(\lambda)$ and v can be either positive or negative. The leading term in Eq. (1) follows the adiabatic approximation at $v \to 0$ and only depends on the instantaneous ground state $|\lambda_\mathrm{f}\rangle$ at the ending point of the ramping.

Since $\left\langle\widehat{O}\right\rangle$ in Eq. (1) is measured under the instantaneous quantum state following the ramping dynamics, $\left\langle\widehat{O}\right\rangle$ should depend on the entire ramping trajectory. However, the main finding of this work is that, under the conditions (1)–(3) mentioned above, the coefficient α of the linear term in Eq. (1) only depends on the quantum state at the ending point and is independent of the starting point λ_i, and other detail of the trajectory. That is to say, the results measured with different ramping trajectories shown in Fig. 1a should collapse into a single straight line in the regime of small v, and the slope of this line determines α, as schematically shown in Fig. 1b. Moreover, we find that α measures the correlation function at the ending point given by

$$\alpha = \mathrm{i}\frac{\partial\mathscr{G}^\mathrm{R}(\omega,\ \lambda_\mathrm{f})}{\partial\omega}|_{\omega=0}. \tag{2}$$

Here $\mathscr{G}^\mathrm{R}(\omega,\ \lambda_\mathrm{f})$ is the Fourier transformation of the retarded Green's function $\mathscr{G}^\mathrm{R}(t,\ \lambda_\mathrm{f})$, and $\mathscr{G}^\mathrm{R}(t,\ \lambda_\mathrm{f})$ is defined as [6]

$$\mathscr{G}^\mathrm{R}(t,\lambda_f) = -\mathrm{i}\Theta(t)\langle\lambda_\mathrm{f}|\left[\hat{O}(t),\ \hat{V}(0)\right]|\lambda_\mathrm{f}\rangle, \tag{3}$$

where $\widehat{V} = \partial\widehat{H}/\partial\lambda$ and $\Theta(t)$ is the step function. In practice, this allows us to experimentally access the equilibrium correlation given by Eq. (2) by ramping to a given final parameter λ_f with various ramping velocities. Since this correlation is obtained by the first order correction away from the adiabatic limit, it is now termed as the non-adiabatic linear response. Note that unlike the conventional linear response that is related to correlation functions, this response is related to the frequency derivative of correlation functions. As we will show below, this correlation function directly probes whether the spectral function is symmetric with respect to positive and negative frequencies and, therefore, provides direct access to the nature of quasi-particle description.

The proof of this result follows straightforwardly from the perturbation expansion in term of ramping velocity, as we show in the Supplementary materials I. In the Supplementary materials II, we also show three examples, including the transverse field Ising model, the fermion pairing model and the Bogoliubov model for bosons. The numerical simulations of the ramping dynamics in these models confirm the consistency between the slope and the correlation function given by Eq. (2). We remark that, although Eqs. (2) and (3) are derived at zero-temperature, we can extend the formula to finite temperature under the condition that the thermalization time scale is much shorter than the ramping time scale. At finite temperature, we use the thermal ensemble average to replace the average over quantum state $|\lambda_\mathrm{f}\rangle$ in Eq. (3).

Here we should note that our theory is a perturbative expansion in terms of v. Therefore, there always exists a convergent regime

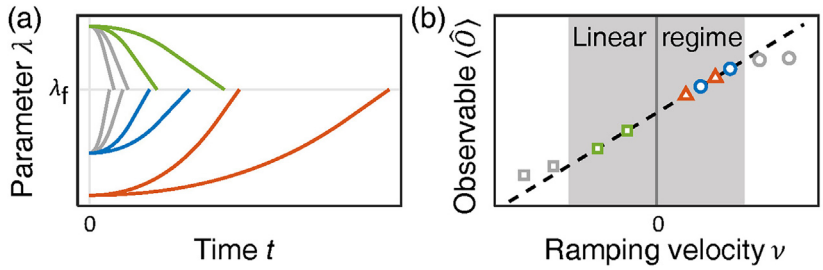

Fig. 1. (Color online) Schematic of the main result. (a) Ramping a parameter λ in Hamiltonian $H(\lambda)$ to the same final value λ_f with different initial values and different ramping velocities v. Measurement $\langle\hat{O}\rangle$ is performed right after the ramping dynamics ends at λ_f. (b) The measured $\langle\hat{O}\rangle$ with various ramping trajectories in terms of ramping velocity v. In the region of small v indicated by the shaded area, all data points collapse into a linear curve and the slope α of the curve only depends on the final value λ_f, independent of initial values and other details of the trajectories. This slope probes the equilibrium correlation at λ_f given by Eq. (2).

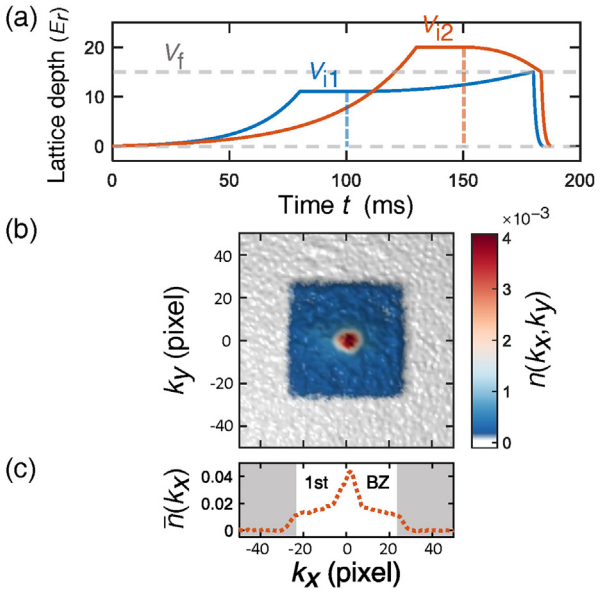

Fig. 2. (Color online) Experimental time sequence and typical results. (a) The time sequence of our experiments. We adiabatically load degenerate ^{87}Rb into optical lattices with different initial lattice depths V_i, such as $V_{i1} = 11E_r$ (blue) and $V_{i2} = 20E_r$ (red) in the illustration. The atoms are hold at the initial lattice depth for 20 ms, and then, we start to ramp the lattices after the time indicated by the dashed lines. After a smoothing procedure at the initial ramping process, we linearly ramp the lattice to the final depth V_f. (b) Typical raw data of the band mapping measurement, resulting in a two-dimensional quasi-momentum distribution $n(k_x, k_y)$. (c) One-dimensional quasi-momentum distribution $\bar{n}(k_x)$ after integration over k_y.

where our theory is valid, as long as the linear order coefficient does not vanish and the higher order coefficients do not diverge, and this condition can be satisfied even for gapless systems. In the low dimension, the low-energy density-of-state is generically high, which leads to a high population of low-energy modes during the ramping dynamics. This leads to the divergence of high-order coefficients, consistent with the discussion of the breakdown of adiabaticity in low-energy gapless systems in the previous literature [32,33]. We discuss the convergence conditions in more detail in the Supplementary materials III. As shown in the Supplementary materials III, if the ramping term and the observable both obey certain symmetry, the linear response will vanish due to the symmetry constraint. Hence, our discussion below always focuses on the cases without such symmetry. Under these conditions, we can always further expand Eq. (1) as

$$\langle\hat{O}\rangle = \langle\lambda_f|\hat{O}|\lambda_f\rangle + \alpha v + \beta v^2 + \ldots, \tag{4}$$

and the validity of the linear expansion at least requires $v \ll \alpha/\beta$. Note that β is not a universal number and is path-dependent. Therefore, the validity range of the linear expansion is path-dependent.

We should also note the difference between our theory and the Kibble-Zurek mechanism. The Kibble-Zurek mechanism focuses on topological defects related to the long-range correlation of order parameters. Therefore, it experiences a critical slowing down at the critical point as it takes a long time to establish a long-range correlation [34,35]. Whereas our theory only concerns local equilibrium, its validity is not affected by the critical slowing down. Hence, our theory can also be applied to ramping across a critical regime.

3. Experimental results

The experiment in the Bose-Hubbard model is carried out with degenerate ^{87}Rb atoms in a three-dimensional optical lattice. The optical lattice is formed by three standing waves perpendicular to each other at wavelength $\lambda = 1064$ nm and the magnetic field is applied along z axis. Each lattice beam has a beam waist of 150(10) μm while the atoms occupy a region with a radius of 13 μm. When the lattice depth is at $5E_r$ ($E_r = h \times 2$ kHz is the recoil energy of the optical lattice), the inhomogeneity of lattice beams provides an external harmonic trap with isotropic radial vibrational frequencies $\sim 2\pi \times 20(1)$ Hz. The ramping time sequence of the experiment is shown in Fig. 3a. We adiabatically load $1.6(1) \times 10^5$ atoms into lattices with an initial lattice depth V_i and hold the system for 20 ms for relaxations. Then we ramp the lattice depth to V_f with a velocity v (in unit of E_r/ms). Here, the starting part of the ramping curve is smoothened to satisfy conditions (1)–(3) discussed above (see the Supplementary materials IV for details). As soon as the lattice depth reaches V_f, we perform the band-mapping measurement [36,37] by imaging the atoms along z-direction, and measure a two-dimensional quasi-momentum distribution $n(k_x, k_y)$ of atoms. A typical result of the band mapping is shown in Fig. 3b. We further integrate $n(k_x, k_y)$ along k_y-direction, which results in a one-dimensional quasi-momentum distribution $\bar{n}(k_x) = \int dk_y n(k_x, k_y)$ as shown in Fig. 3c.

We ramp the lattice depth to the same target value $V_f = 15E_r$ from different initial lattice depths $V_i = 5, 11, 17$ and $20E_r$, and measure $\bar{n}(k_x = 0)$ as a function of v for different V_i. We can see in Fig. 4a that there always exists a linear regime and these linear regimes overlap with each other for trajectories with different V_i. We extract the slope from the linear regime and obtain the slope α of 0.025(2), 0.023(6), 0.024(4) and 0.025(3) for $V_i = 5, 11, 17$ and $20E_r$ respectively as shown in Fig. 4b. We also get α of 0.025(2) and 0.024(2) for $V_i = 18$ and $19E_r$ from data shown in Fig. 4c. Within the statistical errors, it is consistent with our theory that α is independent of the initial lattice depth V_i. Nevertheless, we should note that for different V_i, the window of the linear regime is different. This is because the higher order coefficients in the expansion Eq. (1) depend on the initial value and other details of the trajectories. As the higher order coefficients get

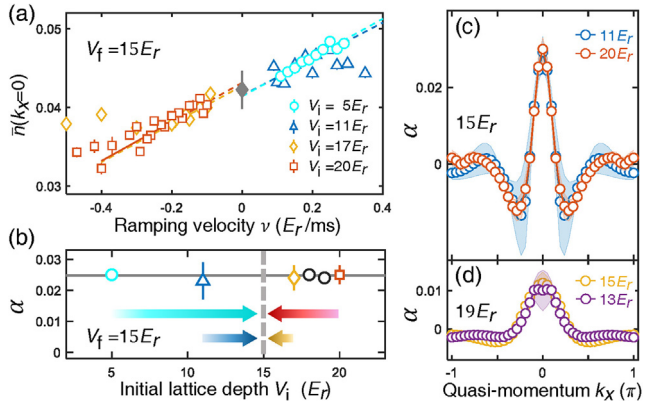

Fig. 3. (Color online) Experimental demonstration of the path independence. (a) $\bar{n}(k_x = 0)$ versus the ramping velocity v. Here we plot four sets of data. The final lattice depth is fixed at $V_f = 15E_r$, and the initial lattice depths are respectively $5E_r$ (cyan circle), $11E_r$ (blue triangle), $17E_r$ (yellow diamond) and $20E_r$ (red square). The error bars here represent one standard errors of the mean by repeating 20 to 80 measurements for each data point. The solid lines are weighted linear fits to the data. The lengths of the solid lines represent the fitting regime and the dashed lines are the extensions of the linear fits. The cyan, blue, yellow, and red lines respectively yield slopes α as 0.025(2), 0.023(6), 0.024(4), and 0.025(3). The grey diamond labels the value of $\bar{n}(k_x = 0)$ by adiabatically ramping to $V_f = 15E_r$ whose error bar denotes one standard deviation of 386 repeating measurements. (b) α versus the initial lattice depth V_i. The horizontal solid line marks the mean value 0.025(1) of α which is obtained by the weighted average of α from six different V_i with $V_i = 5$, 11, 17, 18, 19, and $20E_r$. (c, d) α versus quasi-momentum k_x for the entire first Brillouin zone with $V_f = 15E_r$ (c) and $V_f = 19E_r$ (d). In (c), blue circles represent the situation with $V_i = 11E_r$ and the red circles represent the situation with $V_i = 20E_r$. In (d), yellow circles represent the situation with $V_i = 15E_r$ and the purple circles represent the situation with $V_i = 13E_r$. The shadow areas denote the range of one standard deviation due to statistical errors. The solid lines are guides for eyes.

larger, the linear window gets smaller. We also note that, in the limit of $v \to 0$, data taken with different V_i should give the same result that recovers the adiabatic limit. The small discrepancy in this limit between different data sets (Fig. 4) is due to the day-to-day drift of our experimental apparatus (see the Supplementary materials V).

We verify the path independence of α not only for $\bar{n}(k_x = 0)$ but also for $\bar{n}(k_x)$ in the entire first Brillouin zone. Here, we symmetrize the measured one-dimensional quasi-momentum distributions to extract $\bar{n}(k_x)$ in terms of k_x (see the Supplementary materials VI). Fig. 4c and d show the slope α extracted from $\bar{n}(k_x)$ as a function of k_x. Each plot shows results with the same V_f but two different V_i. One can see that, for the entire first Brillouin zone, $\alpha(k_x)$ with the same V_f and different V_i coincide with each other within the statistical errors.

Then, we vary V_f to probe the correlations at different lattice depths. In Fig. 4a–f, we show results for $V_f = 11$, 13, 15, 17, 19 and $21E_r$. For each given V_f, we ramp the lattice depth to this V_f with at least two different V_i and consistent slopes α are obtained for all cases. In Fig. 4g, we plot α as a function of V_f. We find that α is vanishingly small for $V_f = 11E_r$ and $V_f = 21E_r$, and α is significant for V_f in the range between $13E_r$ and $19E_r$. Note that in our system, the zero-temperature quantum phase transition between the superfluid and the Mott insulator occurs at $13E_r$ for density $n = 1$, $15E_r$ for $n = 2$, and $17E_r$ for $n = 3$ (the local density of our system is up to $n = 3$). Hence, the lattice depth $13E_r - 19E_r$ corresponds to the quantum critical regime in our system.

Therefore, the experimental measurements not only confirm that the non-adiabatic linear response is independent of the details of the ramping trajectories, but also discover that this response is much more significant in the quantum critical regime than that in the superfluid and the Mott insulator phases. To understand this result, we analyze the correlation function probed by Eq. (2) in the Bose-Hubbard model (BHM) below.

4. Application to the Bose-Hubbard model

The Hamiltonian for the BHM is written as

$$\hat{H}_{\mathrm{BHM}} = -J\sum_{\langle ij\rangle}\left(\hat{a}_i^\dagger\hat{a}_j + h.c.\right) + \sum_i\left[\frac{U}{2}\hat{n}_i(\hat{n}_i-1) - \mu\hat{n}_i\right], \tag{5}$$

where $\hat{a}_i$ is the annihilation operator at site-i, $\hat{n}_i = \hat{a}_i^\dagger\hat{a}_i$ is the particle number operator at site-i, J is the hopping strength between neighboring sites, and U is the on-site interaction strength. In the experiment, both J and U change in time during ramping lattice depth. However, since the quasi-momentum distribution is measured in experiments and the measurement operator $\hat{O} = \hat{n}_{\mathbf{k}} = \hat{a}_{\mathbf{k}}^\dagger\hat{a}_{\mathbf{k}}$ commutes with the hopping term, the dominate effect during ramping should come from the changing of parameter U. Hence, for simplicity, we consider ramping the interaction strength U from an initial value U_i to a final value U_f, such that $\partial\hat{H}/\partial\lambda = \sum_i \frac{1}{2}\hat{n}_i(\hat{n}_i - 1)$. Note that the interaction term can also be written in momentum space as

$$\frac{U}{2N_s}\sum_{\mathbf{p},\mathbf{k}_1,\mathbf{k}_2}\hat{a}^\dagger_{\mathbf{p}+\mathbf{k}_1}\hat{a}^\dagger_{\mathbf{p}-\mathbf{k}_1}\hat{a}_{\mathbf{p}-\mathbf{k}_2}\hat{a}_{\mathbf{p}+\mathbf{k}_2}, \tag{6}$$

where N_s is total number of sites. Thus, the non-adiabatic linear response theory presented above probes the correlator

$$\mathscr{G}^{\mathrm{R}}(t,U_f) = \frac{-i\Theta(t)}{2N_s}\sum_{\mathbf{p},\mathbf{k}_1,\mathbf{k}_2}\left\langle\left[\hat{a}^\dagger_{\mathbf{k}}(t)\hat{a}_{\mathbf{k}}(t),\ \hat{a}^\dagger_{\mathbf{p}+\mathbf{k}_1}(0)\hat{a}^\dagger_{\mathbf{p}-\mathbf{k}_1}(0)\hat{a}_{\mathbf{p}-\mathbf{k}_2}(0)\hat{a}_{\mathbf{p}+\mathbf{k}_2}(0)\right]\right\rangle. \tag{7}$$

This correlator is different from density–density or phase correlation measured in the Bose-Hubbard model before [38,39].

We implement the Wick decomposition to express the multiple-points correlation function Eq. (7) in term of two-point correlation functions, where the single-particle spectral function $\mathscr{A}(\mathbf{k},\ \omega)$ can be introduced through the two-point correlation functions as

$$\langle\hat{a}^\dagger_{\mathbf{k}}(t)\hat{a}_{\mathbf{k}'}(0)\rangle = \delta_{\mathbf{k},\mathbf{k}'}\int d\omega f_{\mathrm{B}}(\omega)\mathscr{A}(\mathbf{k},\omega)e^{i\omega t}, \tag{8}$$

$$\langle\hat{a}_{\mathbf{k}}(t)\hat{a}^\dagger_{\mathbf{k}'}(0)\rangle = \delta_{\mathbf{k},\mathbf{k}'}\int d\omega(1+f_{\mathrm{B}}(\omega))\times\mathscr{A}(\mathbf{k},\ \omega)e^{-i\omega t}, \tag{9}$$

and $f_{\mathrm{B}}(\omega) = 1/(e^{\beta(\omega-\mu)}-1)$ is the Bose distribution function (see the Supplementary materials VII and VIII). With this approximation, the correlator Eq. (7), and consequently α given by Eq. (2), is eventually determined by the spectral function $\mathscr{A}(\mathbf{k},\ \omega)$ as

$$\alpha = 4\pi\bar{n}\int d\omega f_{\mathrm{B}}(\omega)\mathscr{A}(\mathbf{k},\ \omega)\frac{\partial}{\partial\omega}\mathscr{A}(\mathbf{k},\ \omega). \tag{10}$$

In the BHM, there are two types of spectral function $\mathscr{A}(\mathbf{k},\ \omega)$ [6]. When the system is either deeply in the superfluid phase or deeply in the Mott insulator phase, the system possesses well-defined quasi-particles. In the case, $\mathscr{A}(\mathbf{k},\ \omega)$ behaves as

$$\mathscr{A}(\mathbf{k},\ \omega) \sim \frac{\Gamma_{\mathbf{k}}}{(\omega-\epsilon_{\mathbf{k}})^2+\Gamma_{\mathbf{k}}^2}, \tag{11}$$

where $\epsilon_{\mathbf{k}}$ is the quasi-particle energy, and $1/\Gamma_{\mathbf{k}}$ gives the quasi-particle lifetime. When the quasi-particle lifetime is long enough, $\Gamma_{\mathbf{k}} \to 0$ and $k_bT \gg \Gamma_{\mathbf{k}}$. Then, $f_{\mathrm{B}}(\omega)$ can be taken as a constant in the energy window $\sim\Gamma_{\mathbf{k}}$ around $\epsilon_{\mathbf{k}}$. Thus, it is easy to see that $A(\mathbf{k},\ \omega)$ is an even function and $\partial A(\mathbf{k},\ \omega)/\partial\omega$ is an odd function centered around $\epsilon_{\mathbf{k}}$. Hence, after the integration, α approaches zero.

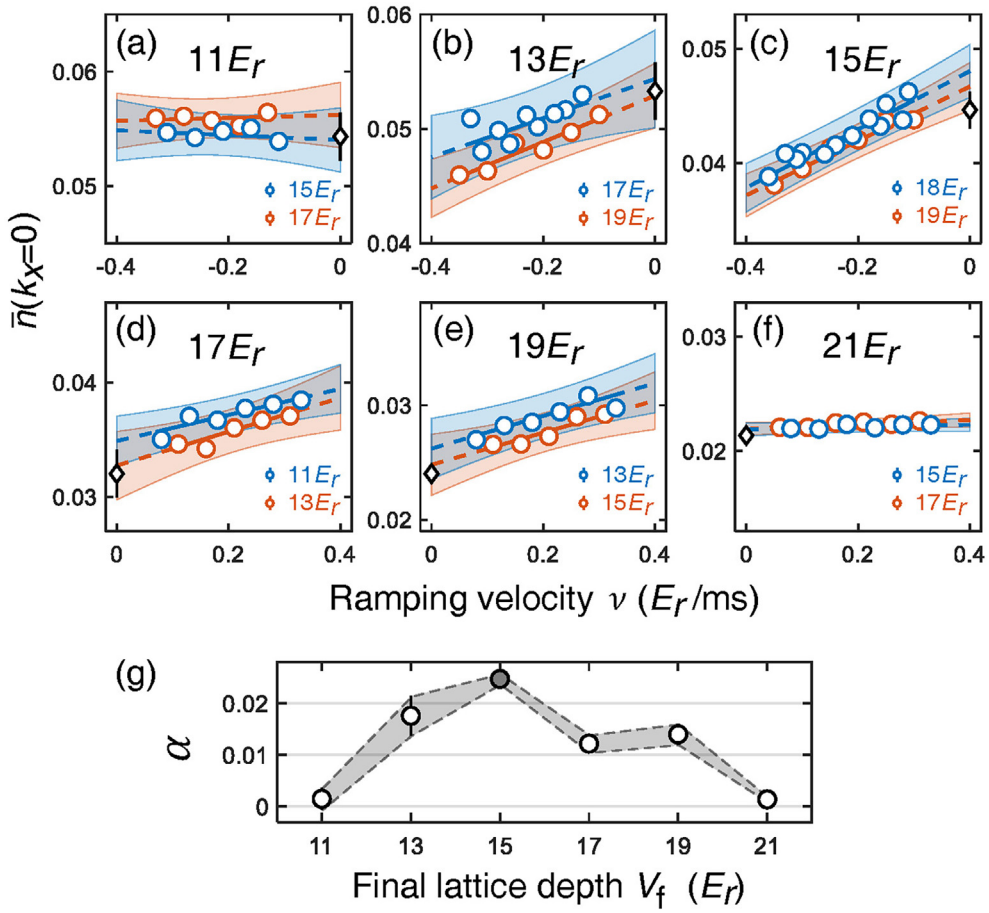

Fig. 4. (Color online) The measured correlation versus the final lattice depth V_f. (a–f) $\bar{n}(k_x = 0)$ versus the ramping velocity v by ramping to a set of different V_f (11, 13, 15, 17, 19, or 21E_r). Each panel shows a fixed V_f with two different initial V_i. The circles are data with error bars (usually smaller than marker size) being one standard error of 20 to 40 repeated measurements. The solid lines are the linear fits, and the dashed lines are the extension of linear fits outside of the measurement ranges. The black diamonds correspond to the adiabatic measurement of $\bar{n}(k_x = 0)$ whose error bars are given by one standard deviation of 15 to 20 repeated measurements. The shadow areas denote the 95% confidence intervals. (g) α versus the final lattice depth V_f. The shadow area shows the uncertainty range of one standard deviation.

When the system is in the critical regime, the system no longer possesses well-defined quasi-particles and $\mathcal{A}(\mathbf{k},\ \omega)$ behaves as

$$\mathcal{A}(\mathbf{k},\ \omega) \sim \frac{\Theta(\omega - \epsilon_{\mathbf{k}})}{(\omega - \epsilon_{\mathbf{k}})^{\eta}}, \tag{12}$$

where η is a critical exponent [6,40]. Substituting Eq. (12) into Eq. (10), it is straightforward to obtain

$$\alpha \propto \frac{n}{T^{2\eta}} f_{\mathrm{B}}(\epsilon_{\mathbf{k}}). \tag{13}$$

This discussion explains the experimental findings presented in Fig. 4, and attributes the difference in the non-adiabatic linear response in this system to whether the quantum phases possess well-defined quasi-particle descriptions or not.

Ideally, by comparing our measurements with Eq. (13), we can determine the critical exponent by studying the temperature dependence of this correlation. However, since our current experiment is performed in the presence of a harmonic trap, the correlation is smeared out by the density inhomogeneity in the real space. This limitation can be lifted by using the box potential in a future experiment.

5. Conclusions and outlook

We find a new regime for many-body dynamics, where the deviations from steady states are independent of the trajectories of dynamics. In this regime, the non-adiabatic response is linear instead of conventional power laws. This provides us with a scheme to probe the many-body systems via universal ramping dynamics, and measure whether the system has well-defined quasi-particle behaviors. Besides the BHM, our scheme can be directly applied to probe correlations in other systems with ultracold atomic gases, such as unitary Fermi gas and quantum simulation of various spin models. Our method can also be applied to other systems beyond ultracold atomic gases, such as trapped ions, NV centers, and condensed matter systems. As demonstrated in studying the Bose-Hubbard model, our method accesses a different aspect of quantum many-body correlation compared with many existing measurement tools. Thus, our protocol provides a new tool for experimentally studying correlations in quantum matters.

Conflict of interest

The authors declare that they have no conflict of interest.

Acknowledgments

This work was supported by Beijing Outstanding Young Scholar Program, the National Key Research and Development Program of China (2021YFA0718303, 2021YFA1400904, and 2016YFA0301501), the National Natural Science Foundation of China (91736208, 11974202, 61975092, 11920101004,

61727819, 11934002, 11734010, and 92165203), and the XPLORER Prize.

Author contributions

Jiazhong Hu, Hui Zhai, Wenlan Chen, and Xuzong Chen supervised this work. Hui Zhai, Wei Zheng, Zhiyuan Yao, and Tiangang Zhou developed the theory. Libo Liang and Ruixiao Yao designed and performed the experiment with the help of Qinpei Zheng and Qi Huang. Libo Liang and Ruixiao Yao analyzed the experimental data and obtained the final results. All authors discussed the results and wrote the manuscript.

Appendix A. Supplementary materials

Supplementary materials to this article can be found online at https://doi.org/10.1016/j.scib.2022.12.005.

References

[1] Sobota JA, He Y, Shen Z-X. Angle-resolved photoemission studies of quantum materials. Rev Mod Phys 2021;93:025006.
[2] Mühlbauer S, Honecker D, Périgo éA, et al. Magnetic small-angle neutron scattering. Rev Mod Phys 2019;91:015004.
[3] Datta S. Quantum transport: atom to transistor. Cambridge: Cambridge University Press; 2005.
[4] Pitaevskii L, Stringari S. Bose-einstein condensation and superfluidity. Oxford: Oxford University Press; 2016.
[5] Zhai H. Ultracold atomic physics. Cambridge: Cambridge University Press; 2021.
[6] Sachdev S. Quantum phase transitions. 2 ed. Cambridge: Cambridge University Press; 2011.
[7] Giamarchi T. Quantum physics in one dimension. Oxford: Oxford University Press; 2003.
[8] Stewart GR. Non-Fermi-liquid behavior in d- and f-electron metals. Rev Mod Phys 2001;73:797–855.
[9] Lee S-S. Recent developments in non-Fermi liquid theory. Ann Rev Cond Matt Phys 2018;9:227–44.
[10] Dao T-L, Georges A, Dalibard J, et al. Measuring the one-particle excitations of ultracold fermionic atoms by stimulated raman spectroscopy. Phys Rev Lett 2007;98:240402.
[11] Stewart JT, Gaebler JP, Jin DS. Using photoemission spectroscopy to probe a strongly interacting Fermi gas. Nature 2008;454:744–7.
[12] Gaebler JP, Stewart JT, Drake TE, et al. Observation of pseudogap behaviour in a strongly interacting Fermi gas. Nat Phys 2010;6:569–73.
[13] Feld M, Fröhlich B, Vogt E, et al. Observation of a pairing pseudogap in a two-dimensional Fermi gas. Nature 2011;480:75–8.
[14] Clément D, Fabbri N, Fallani L, et al. Exploring correlated 1d Bose gases from the superfluid to the Mott-insulator state by inelastic light scattering. Phys Rev Lett 2009;102:155301.
[15] Ernst PT, Götze S, Krauser JS, et al. Probing superfluids in optical lattices by momentum-resolved bragg spectroscopy. Nat Phys 2010;6:56–61.
[16] Fabbri N, Huber SD, Clément D, et al. Quasiparticle dynamics in a Bose insulator probed by interband Bragg spectroscopy. Phys Rev Lett 2012;109:055301.
[17] Thouless DJ. Quantization of particle transport. Phys Rev B 1983;27:6083–7.
[18] Niu Q, Thouless DJ. Quantised adiabatic charge transport in the presence of substrate disorder and many-body interaction. J Phys A Math Gene 1984;17:2453.
[19] Lohse M, Schweizer C, Zilberberg O, et al. A Thouless quantum pump with ultracold bosonic atoms in an optical superlattice. Nat Phys 2016;12:350–4.
[20] Nakajima S, Tomita T, Taie S, et al. Topological Thouless pumping of ultracold fermions. Nat Phys 2016;12:296–300.
[21] Kibble TWB. Topology of cosmic domains and strings. J Phys A Math Gene 1976;9:1387.
[22] Kibble TWB. Some implications of a cosmological phase transition. Phys Rep 1980;67:183–99.
[23] Zurek W. Cosmological experiments in superfluid helium? Nature 1985;317:505–8.
[24] Zurek WH, Dorner U, Zoller P. Dynamics of a quantum phase transition. Phys Rev Lett 2005;95:105701.
[25] Chen D, White M, Borries C, et al. Quantum quench of an atomic Mott insulator. Phys Rev Lett 2011;106:235304.
[26] Braun S, Friesdorf M, Hodgman SS, et al. Emergence of coherence and the dynamics of quantum phase transitions. Proc Natl Acad Sci USA 2015;112:3641–6.
[27] Clark LW, Feng L, Chin C. Universal space-time scaling symmetry in the dynamics of bosons across a quantum phase transition. Science 2016;354:606–10.
[28] Anquez M, Robbins BA, Bharath HM, et al. Quantum Kibble-Zurek mechanism in a spin-1 Bose-einstein condensate. Phys Rev Lett 2016;116:155301.
[29] Keesling A, Omran A, Levine H, et al. Quantum Kibble-Zurek mechanism and critical dynamics on a programmable Rydberg simulator. Nature 2019;568:207–11.
[30] Ko B, Park JW, Shin Y. Kibble-Zurek universality in a strongly interacting Fermi superfluid. Nat Phys 2019;15:1227–31.
[31] Liu X-P, Yao X-C, Deng Y, et al. Dynamic formation of quasicondensate and spontaneous vortices in a strongly interacting Fermi gas. Phys Rev Res 2021;3:043115.
[32] Polkovnikov A. Universal adiabatic dynamics in the vicinity of a quantum critical point. Phys Rev B 2005;72:161201.
[33] Polkovnikov A, Gritsev V. Breakdown of the adiabatic limit in low-dimensional gapless systems. Nat Phys 2008;4:477–81.
[34] Zurek WH. Cosmological experiments in condensed matter systems. Phys Rep 1996;276:177–221.
[35] del Campo A, Zurek WH. Universality of phase transition dynamics: topological defects from symmetry breaking. Int J Mod Phys A 2014;29:1430018.
[36] Kohl M, Moritz H, Stoferle T, et al. Fermionic atoms in a three dimensional optical lattice: observing Fermi surfaces, dynamics, and interactions. Phys Rev Lett 2005;94:080403.
[37] Huang Q, Yao R, Liang L, et al. Observation of many-body quantum phase transitions beyond the Kibble-Zurek mechanism. Phys Rev Lett 2021;127:200601.
[38] Endres M, Cheneau M, Fukuhara T, et al. Observation of correlated particle-hole pairs and string order in low-dimensional Mott insulators. Science 2011;334:200–3.
[39] Gring M, Kuhnert M, Langen T, et al. Relaxation and prethermalization in an isolated quantum system. Science 2012;337:1318–22.
[40] Endres M, Fukuhara T, Pekker D, et al. The "Higgs" amplitude mode at the two-dimensional superfluid/Mott insulator transition. Nature 2012;487:454–8.

Libo Liang is currently a Ph.D. student at the School of Electronics, Peking University. He got his bachelor's degree from the School of Physics, Peking University. His research focuses on quantum precision measurements and quantum simulations, including ultracold quantum gases and quantum many-body correlations.

Wei Zheng is an assistant professor of physics at University of Science and Technology of China. He got both bachelor's and doctor's degrees from Sun Yat-sen University. He works in theoretical quantum many-body physics, including ultracold atomic gases, condensed matters, and non-equilibrium phenomena.

Ruixiao Yao is currently a Ph.D. student at the Physics Department, the Massachusetts Institute of Technology (MIT). He got his bachelor's degree from Peking University, and later worked at Tsinghua University as a research scientist. His research focuses on quantum many-body physics including ultracold quantum gases, strongly correlated system, and quantum information science.

Xuzong Chen is a professor at the Institute of Quantum Electronics, Peking University. He is currently head of the Laboratory of Space Ultracold Atoms at Peking University. His research topics include fundamentals of quantum science and quantum technology, space cold atomic physics, multi-body quantum physics, Bose Einstein condensation, Bose Fermi mixing, quantum simulation, and novel atomic cesium clock.

Wenlan Chen is an associate professor at Department of Physics, Tsinghua University. She received her Ph.D. degree in Physics from MIT with the award of Martin Deutsch Prize in 2015. She continued the postdoctoral research at MIT from 2015 to 2018. Her team at Tsinghua University is now focusing on experimental quantum physics with the platform of ultracold atoms and high-cooperativity cavities. Her research interest is quantum computation, quantum simulation, and quantum many-body physics.

Hui Zhai is a full professor at Institute for Advanced Study of Tsinghua University. He got both his Bachelor's and Doctor's degrees from Tsinghua University. His work mainly focuses on the theory of quantum matters, including cold atomic gases, holographic quantum matters and machine learning applications in quantum physics.

Jiazhong Hu is an associate professor at Tsinghua University, and he obtained the Doctor of Philosophy in AMO Physics from MIT in 2017. Now he is leading a new experimental team working in ultracold atoms and developing novel quantum techniques, and his research interest mainly focuses on quantum simulations and many-body physics.